Nanostructured YSZ thermal barrier coatings engineered to counteract sintering effects

Lima, R. S.; Marple, B. R.

Publisher's version / Version de l'éditeur:
https://doi.org/10.1016/j.msea.2007.07.082
Materials Science and Engineering A, 485, 1-2, pp. 182-193, 2008-06-25

ELSEVIER

Materials Science and Engineering A 485 (2008) 182–193

MATERIALS SCIENCE & ENGINEERING A

www.elsevier.com/locate/msea

Nanostructured YSZ thermal barrier coatings engineered to counteract sintering effects

R.S. Lima *, B.R. Marple

National Research Council of Canada, 75 de Mortagne Blvd., Boucherville, Que. J4B 6Y4, Canada

Received 29 May 2007; received in revised form 24 July 2007; accepted 26 July 2007

Abstract

Thermal spray zirconia–8 wt% yttria (YSZ) deposits have been employed as thermal barrier coatings (TBCs) in the hot sections of gas turbines. The use of nanostructured YSZ represents an alternative for improving the performance of these coatings. Despite some initial positive research results, there are still fundamental questions to be answered on the applicability of nanostructured YSZ coatings as TBCs. These questions are related to sintering effects, which could significantly increase the thermal diffusivity/conductivity and elastic modulus values of these types of coatings in high temperature environments. In this study, nanostructured and conventional YSZ coatings were heat-treated at 1400 °C for 1, 5 and 20 h. It was observed that the nanostructured coatings counteract sintering effects, due to the presence of a bimodal microstructure exhibiting regions with different sintering rates: (i) matrix (low rate) and (ii) nanozones (high rate). Important sintering-affected properties, like thermal diffusivity and elastic modulus were studied. The thermal diffusivity and elastic modulus values of the nanostructured YSZ coatings were significantly lower than those of conventional YSZ coatings, even after an exposure to a temperature of 1400 °C for 20 h. This study demonstrates that nanostructured YSZ coatings can be engineered to counteract sintering effects and exhibit significantly lower increases in thermal diffusivity and elastic modulus values in high temperature environments when compared to those of conventional YSZ coatings.

Keywords: Thermal spray; Nanostructured ZrO_2–8 wt% Y_2O_3; Thermal barrier coatings (TBCs); Elastic modulus; Thermal diffusivity; Heat treatment; Differential sintering

1. Introduction

1.1. Thermal barrier coatings (TBCs)

Thermal barrier coatings (TBCs) have been employed for many years to protect the metallic components (e.g., combustion cans, blades and vanes) of the hot sections of aerospace and land-based gas turbines against the high temperature environment. The state-of-the-art TBC system is currently formed by a metallic bond coat (e.g., CoNiCrAlY) and a zirconia–yttria (ZrO_2–7–8 wt% Y_2O_3) (YSZ) top coat [1,2]. The typical thicknesses of TBCs vary between 100 and 500 μm, and they can provide a major reduction in the surface temperature of the metallic components of up to 300 °C, when combined with the use of internal air cooling of the underlying metallic component. Due to this characteristic, TBCs allow gas turbine engines to operate at temperatures higher than that of the melting point of the metallic components of turbines (superalloys), which is approximately 1300 °C. Therefore, TBCs enable an increase in the efficiency and performance, and a reduction in the pollution levels of these types of engines [1,2]. Ceramic coatings were first applied as TBCs during the 1960s in the nozzles of the X-15 rocket planes and they became a standard product for commercial gas turbines in the 1980s [1]. Air plasma spray (APS) and electron beam physical vapour deposition are the two main processing techniques used to deposit YSZ coatings today for TBC applications [2].

1.2. Nanostructured materials and TBCs

Nanoscience and technology offer the potential for significant advances in the performance of new and established materials based on improvements in physical and mechanical properties resulting from reducing the grain size by factors from 100 to 1000 times when compared to current engineering materials. Nanostructured materials exhibit grain (particle) sizes that are less than 100 nm in at least one dimension [3]. In addition to

* Corresponding author. Tel.: +1 450 641 5150; fax: +1 450 641 5105.
E-mail address: rogerio.lima@cnrc-nrc.gc.ca (R.S. Lima).

0921-5093/$ – see front matter.
doi:10.1016/j.msea.2007.07.082

research in bulk samples, the study of nanostructured materials has also been extended to the area of surfaces and coatings, including thermal spray coatings [4]. The possibility of engineering coatings with superior wear resistance and more durable TBCs when compared to the conventional thermal spray coatings currently available opens a wide range of research and industrial application opportunities.

Initial studies on nanostructured air plasma sprayed YSZ coatings have shown that it is paramount to carefully control the spray parameters to avoid the complete melting of the nanostructured YSZ agglomerates in the plasma jet to preserve and embed part of the nanostructure of the agglomerates into the coating microstructure. Those coatings were produced from microscopic porous spray-dried particles formed via the agglomeration of individual nanosized YSZ particles. The semi-molten agglomerates, once embedded in the coating microstructure, created a bimodal feature, which consisted of a structure formed by the resolidification of agglomerates that had been fully molten in the spray jet combined with zones resulting from the incorporation of semi-molten material. By controlling the amount of previously molten and porous semi-molten particles embedded in the coating microstructure, it was possible to change considerably the mechanical response of the coating. Therefore, this bimodal microstructure affected the mechanical behaviour of the coating [5–7]. For example, under scratch testing monitored via acoustic emission (AE), it was observed that conventional YSZ coatings exhibited a larger number of AE events when compared to those of nanostructured YSZ coatings [8]. It was also observed that on average, the transversal load during scratch testing exerted by the nanostructured coating that exhibited the highest amount of previously semi-molten porous nanoagglomerates embedded in the coating microstructure, was significantly lower than that of the conventional YSZ coatings [8]. Therefore it was concluded that the nanostructured coatings exhibited improved compliance characteristics.

More recently, thermal shock tests were carried out for air plasma sprayed nanostructured YSZ coatings produced from agglomerated powders. Liang and Ding evaluated the thermal shock resistance of nano and conventional YSZ coatings by heating them in a furnace for 30 min at a series of temperatures up to 1300 °C, followed by subsequent cooling (dropping) in cool water for 10 min. For the thermal shock tests carried out at temperatures from 1000 to 1300 °C, the number of cycles to failure of the nano YSZ coatings was approximately 2–3 times higher than that of the conventional coatings [9]. Wang et al. also evaluated the thermal shock resistance of nano and conventional (fused and crushed powder) TBCs. The coatings were heated to 1200 °C for 5 min in a furnace and quenched in water at room temperature. The number of cycles to failure of the nanostructured YSZ coating was 2–4 times higher than that of the conventional coating [10]. These results also demonstrate the higher compliance capabilities of the nanostructured YSZ coatings.

These studies are encouraging; however, there is a skepticism in the thermal spray scientific community about the applicability of these coatings as TBCs. It is hypothesized that these nanostructured YSZ coatings would exhibit sintering (densification) rates much superior to those of conventional YSZ coatings once exposed to the high temperature environment of gas turbines. These high densification rates would increase the thermal diffusivity/conductivity and elastic modulus values (coating stiffening) of the nanostructured YSZ coatings to above critical levels, thereby impeding the application of this type of coating in a TBC system or leading to its premature failure.

The objective of this work is to show that it is possible to engineer novel air plasma spray coating microstructures from nanoagglomerated YSZ powders that can counteract sintering (densification) effects, which will impede the significant increase of thermal diffusivity/conductivity and elastic modulus values in high temperature environments, keeping them at levels even lower than those of conventional YSZ coatings.

2. Experimental procedure

2.1. Feedstock powders

The nanostructured YSZ (ZrO_2–7 wt% Y_2O_3) (Nanox S4007, Inframat Corporation, Farmington, CT, USA) powder was produced by the manufacturer via spray-drying by agglomerating individual nanosized YSZ into microscopic agglomerates, suitable for being fed and thermally sprayed using conventional thermal spray powder feeders. The nanostructured YSZ agglomerated powder received from the manufacturer exhibited a nominal particle size distribution ranging from approximately 15 to 150 μm. Sieving was employed to remove smaller particles from the initial size distribution to produce a distribution containing coarser particles. The 15–150 μm powder was sieved using a 53 μm (Mesh 270) USA Standard Testing Sieve and sieving equipment (Alpine Augsburg Vacuum Sifter, Germany) in to order to try to obtain a particle size range of approximately 50–150 μm [11].

The conventional YSZ (ZrO_2–8 wt% Y_2O_3) (Metco 204B-NS, Sulzer Metco, Westbury, NY, USA) powder had been spray-dried and plasma-densified forming the so-called hollow spherical powder (HOSP). According to the manufacturer, this powder exhibited a nominal particle size distribution varying from 45 to 75 μm. Because this powder is widely used worldwide as feedstock for the production of TBCs, it is considered as representative of currently used standard conventional YSZ material employed for TBC applications.

The particle size distribution of both powders was evaluated by a laser diffraction particle size analyzer (Beckman Coulter LS 13320, Beckman Coulter, Miami, FL, USA). The nanostructural and microstructural characteristics of the nanostructured YSZ powder were evaluated via scanning electron microscopy (SEM).

2.2. Thermal spraying and deposition efficiency (DE)

The nanostructured YSZ powder was thermally sprayed using an Ar/H_2 APS torch (F4-MB, Sulzer Metco, Westbury, NY, USA). The conventional YSZ powder was also air plasma sprayed (Ar/H_2), however, a different torch (9-MB (GH nozzle), Sulzer Metco, Westbury, NY, USA) was employed. The

conventional powder was sprayed based on the standard parameters suggested by the manufacturer of the powder and torch (i.e., Sulzer Metco) [12]. The overall spray conditions/parameters used to deposit the nanostructured YSZ coating were developed internally [11]. The coatings were deposited by a robot on low carbon steel substrates that had been grit-blasted to roughen the surface before spraying.

Initially during plasma spraying (before coating deposition), the velocities and temperatures of the YSZ particles in the spray jet were measured using a diagnostic tool (Accuraspray, Tecnar Automation, Saint Bruno, QC, Canada). The diagnostic tool is based on optical pyrometry and time-of-flight measurements to measure the distribution of particle temperature and velocity in the thermal spray jet. The particle detector was placed at the same spray distance as used when depositing the coatings, i.e., 10 and 11 cm from the torch nozzle for the nanostructured and conventional YSZ coatings, respectively. During the spraying process, a cooling system (air jets) was applied to reduce the coating temperature, which was monitored using a pyrometer. The maximum surface temperature was approximately 160 °C for the both types of YSZ coatings. The thicknesses of the coatings varied from 450 to 550 μm. It is important to point out that both YSZ powders were sprayed using standard thermal spray equipment, i.e., no special torch nozzles, injectors or powder feeders were employed.

The value of deposition efficiency (DE) was also measured by depositing on a grit-blasted low carbon steel substrate of known dimensions using a pre-determined powder feed rate, torch speed, and total number of passes, and then comparing the weight of the substrate before and after the deposition with respect to the feedstock feed rate. The powder feed rate used for DE measurements and coating deposition was 30 g/min, for both powders.

2.3. Heat treatment

A heat treatment was performed on both types of coatings to determine the effect of temperature on the microstructure, thermal diffusivity and elastic modulus values. The heat treatment was carried out on free-standing coatings that had been removed from the low carbon steel substrates by dissolving the metal base. The heat treatment was carried out in a furnace in air by commencing at room temperature and increasing to 1400 °C over a 60–90 min period. The coatings were left at this temperature for a dwell time of 1, 5 and 20 h. After each period, the samples were removed from the furnace and allowed to cool. Initial cooling was very rapid and, typically, room temperature was reached within 30 min.

2.4. Thermal diffusivity

The thermal diffusivity values of as-sprayed and heat-treated coatings were determined by a laser flash method. The measurements were made on coatings that had been removed from the substrate. More details on how this technique can be employed to evaluate the thermal diffusivity of thermal spray coatings can be found elsewhere [13].

It is important to point out that, for the nanostructured and conventional YSZ, all thermal diffusivity samples were sprayed in the same batch. This was done to guarantee that the initial microstructure of the as-sprayed samples (and the samples that were subsequently subjected to heat treatment) was uniform. In addition, to ensure uniformity, as previously stated in Section 2.2, all coatings were deposited by a robot. Each diffusivity sample (coating) exhibited a thickness of ∼500 μm and a diameter of 8 mm. Round samples used for thermal diffusivity measurements via the laser flash method generally exhibit diameters varying from 6 to 12 mm. This is done to match the diameter of the laser beam (yttrium aluminium garnet-YAG-based) used to heat the specimen and sample a representative part of a uniform material. Just one sample per as-sprayed and heat-treated coating was measured.

2.5. Elastic modulus

The elastic modulus values of the as-sprayed and heat-treated nanostructured and conventional coatings were also measured on samples that had been removed from the substrate. The elastic modulus values were measured on the in-plane direction of the coating, also referred to as C_{11}. This technique generates ultrasonic waves by a Nd:YAG (third harmonic: 355 nm) laser pulse focused in a line (∼200 μm × 5 mm) in the coating surface. The waves were detected about 6 mm away in the same surface by a long pulse Nd:YAG (1064 nm) also focused in a line geometry. The scattered detection light was demodulated by a GaAs photorefractive interferometer. By measuring the arrival time of the fundamental symmetry wave mode (S0), the elastic constant could be calculated. The same approach was employed to determine the elastic modulus values of as-sprayed and heat-treated coatings. It must be noted that the elastic modulus values reported in this work should not be taken as absolute. They allow comparison of the different coatings and provide a basis for determining the relative effect of the various heat treatments on the elastic properties. Other examples on how this technique can be employed to evaluate the elastic modulus of thermal spray coatings can be found elsewhere [14].

To assure coating uniformity the approach outlined in Section 2.4 for the thermal diffusivity samples was also used for the production of the elastic modulus samples. The elastic modulus samples exhibited a width of 2.5 cm, a length of 5 cm and a thickness of ∼500 μm. This 12.5 cm^2 of area fairly represents the overall structure of a uniform thermal spray coating. Just one sample per as-sprayed and heat-treated coating was employed for the evaluation of elastic modulus.

As previously stated, the elastic modulus was determined by measuring the velocity of an elastic wave generated by a laser ultrasound in the coating. To determine the elastic modulus using this velocity value the coating density is needed. In this study, the same value of coating density (4.7 g/cm^3) was employed for all coatings when making this calculation. Therefore, the values of elastic modulus reported in later sections must not be taken as absolute; rather, the data allows comparison of the different coatings and provides a basis for determining the relative effect of the various heat treatments on the elastic properties.

2.6. Nano and microstructural evaluation

The structural characteristics of the cross-sections of as-sprayed and heat-treated nanostructured and conventional YSZ coatings were also evaluated by SEM. In order to better preserve and reveal the true structural features of these coatings, they were first vacuum impregnated and mounted in low viscosity epoxy resin, then cut using a diamond saw. Subsequently, they were remounted in epoxy resin using vacuum impregnation and polished using standard metallographic procedures for these types of coatings. The porosity of these coatings was evaluated by using SEM and image analysis on the cross-sections. A total of 10 pictures of each as-sprayed and heat-treated coating were taken (at 500×) to evaluate their respective porosity levels. In order to ensure uniformity of porosity measurements, (i) the pictures of the cross-sections of all coatings were taken at the same SEM conditions and (ii) during image analysis the porosity levels of all coatings were evaluated using the same threshold levels. The amount of previously semi-molten nanoagglomerates embedded in the microstructure of the as-sprayed nanostructured YSZ coating, based on cross-section area, was also measured via SEM and image analysis. A total of 10 pictures of the as-sprayed coating were taken (at 500×) to evaluate the percentage of previously semi-molten particles. By using image analysis (Image Tool software), the nanozones were manually selected and their percentage in area in each of the 10 microstructures was determined.

3. Results and discussion

3.1. Particle size distribution

Fig. 1 shows the particle size distribution (in volume) of the nanostructured (sieved) and conventional YSZ powders. The nanostructured agglomerated powder, after being sieved, exhibits overall particle size distribution varying from ~40 to 160 μm. The average particle diameter is approximately 90 μm. It is important to point out that thermal spray powders exhibit, in general, a particle size distribution range varying within 10–100 μm. This large particle cut of the nanostructured YSZ feedstock was specially tailored to engineer novel YSZ coating microstructures [11], as shown in the next sections. The conventional YSZ powder exhibited a particle size distribution within a normal thermal spray range, i.e., from ~35 to 100 μm, with few particles (in volume) reaching diameters up to ~150 μm. The average particle diameter is approximately 60 μm.

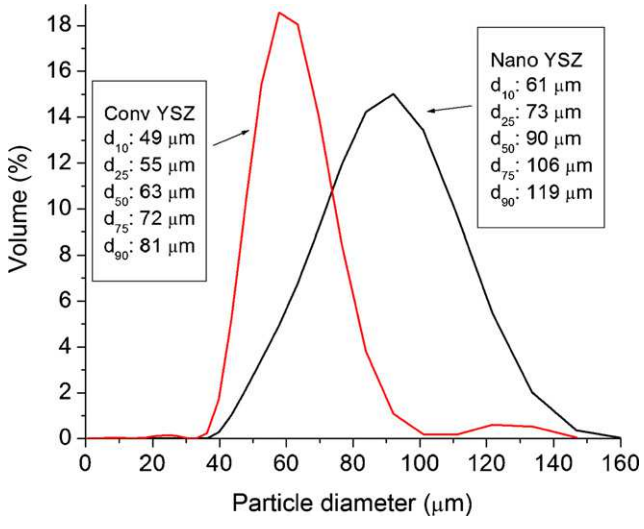

Fig. 1. Particle size distribution of the nanostructured (sieved) and conventional YSZ powders.

3.2. Nanostructural characteristics of the feedstock

Fig. 2 shows SEM pictures of the nanostructured YSZ powder [4]. It is possible to observe that the particle is spherical (Fig. 2a), which is a typical characteristic of spray-dried particles. When examined at higher magnifications it is possible to observe that the particle is porous and formed by the agglomeration of individual nanosized YSZ particles with diameters varying from approximately 30 to 130 nm (Fig. 2b).

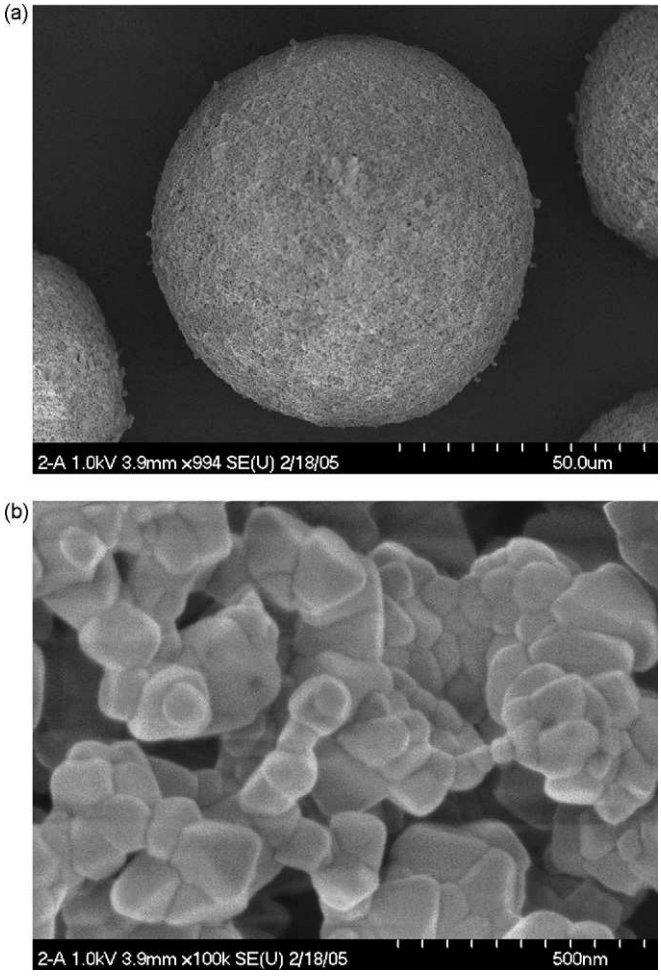

Fig. 2. (a) YSZ feedstock particle formed by the agglomeration (spray-drying) of individual nanosized particles of YSZ [4]. (b) Particle of (a) observed at higher magnification showing individual nanosized YSZ particles (30–130 nm) [4] (scale bar: number represents combined distance across all tick divisions).

As previously stated in Section 2.1, the conventional YSZ powder was spray-dried and plasma-densified forming the so-called hollow spherical powder (HOSP). SEM pictures of this type of HOSP powder can be found elsewhere [7,15].

3.3. In-flight particle characteristics

The average surface temperature and velocity of the thermally sprayed nanostructured YSZ particles were 2670 °C and 210 m/s, respectively. This temperature is below the melting point of ZrO_2–7 wt% Y_2O_3, reported to be approximately 2700 °C [16]. Therefore it is expected that the spray jet impinging the substrate was comprised of fully molten, semi-molten and even non-molten particles. This resulted in part of the nanostructure of the nano YSZ powder being preserved and embedded in the coating microstructure, as shown in Fig. 3. The average surface temperature and velocity of the thermally sprayed conventional YSZ particles were 2700 °C and 148 m/s, respectively.

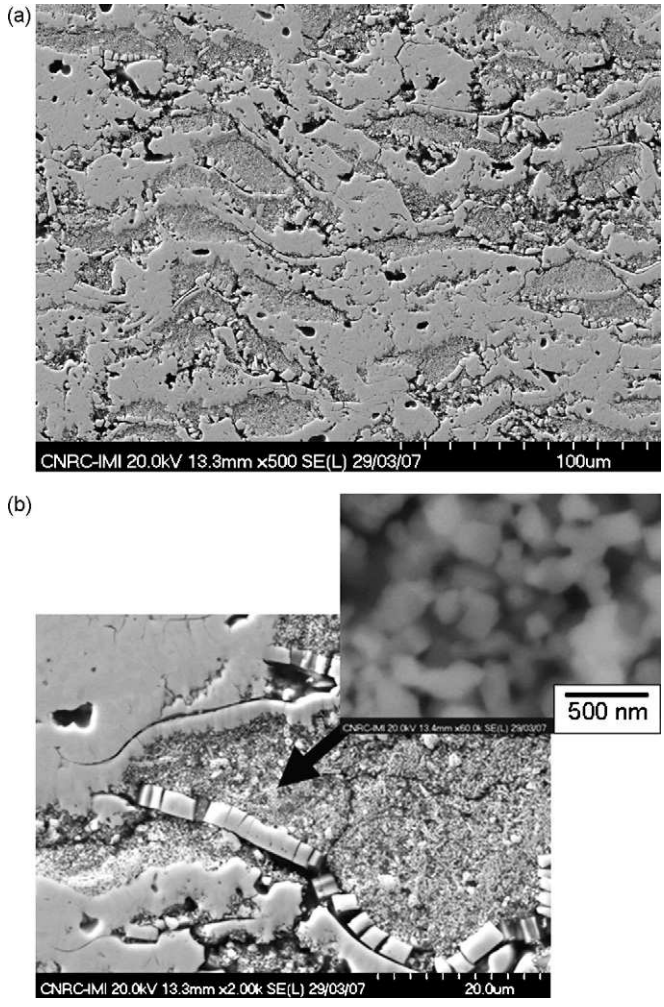

Fig. 3. (a) Microstructure (cross-section) of the nanostructured YSZ coating made from a nanostructured feedstock (Fig. 2). (b) Higher magnification of (a) darker-colored regions containing the previously semi-molten feedstock particles (scale bar: number represents combined distance across all tick divisions).

3.4. Microstructures of the as-sprayed coatings

3.4.1. Nanostructured YSZ coating

Fig. 3 shows the microstructure of the coating produced by using the nanostructured agglomerated YSZ feedstock particles presented in Fig. 2. It is possible to distinguish a bimodal microstructure formed by lighter-colored and darker-colored zones in the coating microstructure (Fig. 3a). When looking at one of the darker-colored regions at higher SEM magnifications (Fig. 3b) it is possible to recognize the similarities between this type of zone and the morphology of the nano YSZ powder (Fig. 2b). The zones like those shown in Fig. 3b correspond to previously semi-molten nanostructured agglomerated YSZ particles that became embedded in the coating microstructure. Zones like those represented in Fig. 3b are also called "nanozones". The lighter-colored zones observed in Fig. 3a probably represent particles that were fully molten in the plasma jet. Therefore, as already observed [6,7], the previously semi-molten YSZ particles are surrounded by a matrix formed by the previously molten YSZ particles, thereby maintaining coating integrity.

It is important to point out that by controlling the size, shape, and morphology of the nanozones it is possible to engineer coatings with very pronounced differences in microstructural characteristics and mechanical performance [4]. A key parameter for TBC development is the density of the nanozones, because they increase the porosity content of the coatings. Based on Fig. 2, it is clear that the nanostructured agglomerated particles comprising the feedstock are porous. Depending on thermal processing, spraying conditions and feedstock characteristics (e.g., diameter), the nanozones that form the coating may continue to be porous like the original feedstock (such as those of Fig. 3b). The porous nanozones are expected to occur when the molten part of the agglomerated semi-molten particle does not fully infiltrate into its non-molten core during thermal spraying [4].

According to McPherson [17], air plasma sprayed ceramic coatings exhibit a bimodal distribution of porosity, with coarse pores in the size range 3–10 μm and fine pores around 100 nm. The coarse porosity is associated with defects in the coating structure, due to incomplete filling of interstices among previously deposited particles, mainly when the impacting particles are not fully molten, whereas, the fine pores are interpreted as incomplete contact between two piled up splats occurring during the process of coating formation.

Based on Fig. 3 it is possible to observe that the nanostructured YSZ coating exhibits a trimodal distribution of porosity, i.e., the bimodal porosity described by McPherson [17], plus the porosity associated with the nanozones (Fig. 3b). The addition of this extra source of porosity will lower the thermal diffusivity and elastic modulus values of this coating, as shown in the next sections.

The percentage of cross-sectional area of previously semi-molten nanoagglomerates embedded in the coating microstructure was estimated to be 35% (Fig. 3a). It is important to highlight that tailoring the nanostructured YSZ powder, through sieving to create a large cut (Fig. 1), was paramount for engineering this novel type of microstructure [11]. As previously

stated, the formation of porous nanozones is expected to occur when the molten part of the agglomerated semi-molten particles do not fully infiltrate into their non-molten cores during thermal spraying. Therefore, to engineer a microstructure containing an effective amount of these porous nanozones it is necessary to (i) spray large agglomerates, (ii) at surface temperatures near the melting point of the material and (iii) at high particle velocities [4].

The large particles (i.e., large volume) will tend to impede full particle melting and limit complete infiltration of the molten part of the particle into the porous inner core (capillaries) during thermal spraying. Surface temperatures near that of the melting point of the material will also tend to avoid the complete melting of the particles during thermal spraying [4,11]. High particle velocity levels are necessary to achieve particle adhesion, cohesion and sufficiently high DE values. Otherwise, these large particles, with average diameter of almost 100 μm (Fig. 1), and average surface temperatures (2670 °C) in the vicinity of the melting point of the YSZ material (~2700 °C [16]), would probably not exhibit sufficient high adhesion/cohesion strength to become embedded in the coating microstructure, i.e., they would tend to bounce off the deposit during thermal spraying.

The average particle velocity levels for YSZ particles sprayed using regular Ar/H_2 air plasma spray torches are normally below 150 m/s when the particle detector is placed at the same spray distance as used when depositing the coatings [12,18]; whereas, the average particle velocity for the nanostructured YSZ particles in this work was 210 m/s. This high average particle velocity probably counteracted the large size (mass) and the borderline surface temperature of the semi-molten particles, allowing a fraction of them to deform, adhere and embed in the coating microstructure (Fig. 3). In fact, the DE value for the nanostructured YSZ powder was 36%, whereas, it was 29% for the conventional YSZ powder, i.e., the DE of the nanostructured powder was not compromised. The higher particle velocity level reached by the nanostructured YSZ particles was mainly the result of using higher H_2 and Ar plasma gas flows in the APS torch, compared to those generally used.

3.4.2. Conventional YSZ coating

Fig. 4 shows the microstructure of the conventional coating. It is possible to observe the typical characteristics of conventional YSZ coatings produced by regular APS torches, i.e., previously molten particles forming lamellar structures (particle spreading at impact) exhibiting globular and intersplat pores, in addition to the presence of microcracks [19]. The average surface temperature of the conventional YSZ powder was basically the same as that of the melting point of YSZ (~2700 °C [16]). Despite that, the microstructure is considerably different from that of the nanostructured YSZ coating (Fig. 3).

It is important to point out that spray-dried and plasma-densified powders (conventional YSZ) are generally comprised of hollow or dense spherical powder particles [7,15]. The hollow particles will tend to exhibit a relatively dense outer shell facilitating heat transfer from the plasma jet to the inner part of the particles and thereby leading to more uniform heating and complete melting of the particle. The same concept can be applied

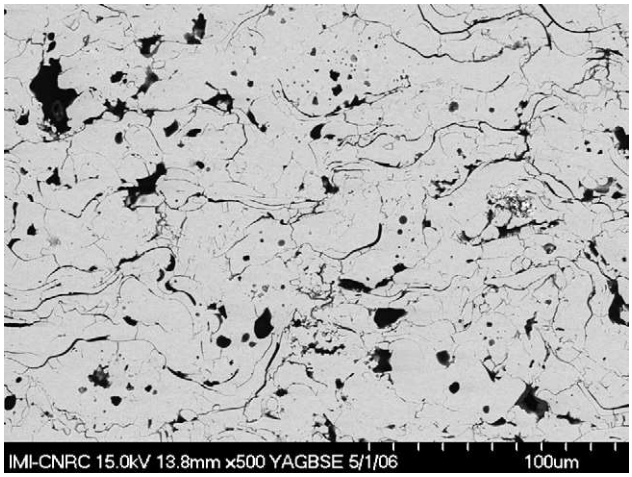

Fig. 4. Microstructure (cross-section) of the conventional YSZ coating (scale bar: number represents combined distance across all tick divisions).

to the dense spherical particles. In addition, the smaller average particle size of the conventional particles, when compared to that of the nanoagglomerates (Fig. 1), will probably tend to facilitate particle melting due to their smaller volumes. Therefore, the majority of the conventional particles that impinge, adhere and embed in the coating microstructure probably consist of fully molten or almost fully molten particles, forming a microstructure with different features from that of the nanostructured YSZ coating. It should be emphasized that the porosity of the nanostructured YSZ powder particles (Fig. 2) during thermal spraying plays the same role as the porosity in a TBC, i.e., the porosity may create a barrier against heat transfer from the plasma jet to the inner core of the particles, making it more difficult for them to melt completely.

3.5. Porosity

Fig. 5 shows the porosity values for nanostructured and conventional YSZ coatings in the as-sprayed state and following

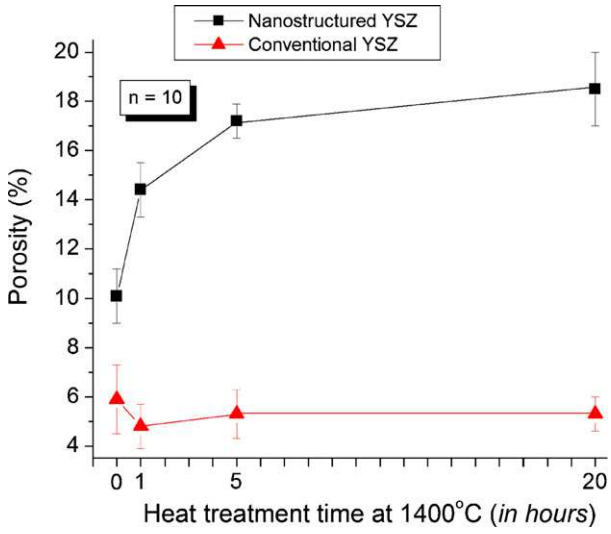

Fig. 5. Variation of the porosity values from as-sprayed to heat-treated nanostructured and conventional YSZ coatings at 1400 °C for 1, 5 and 20 h.

heat treatment at 1400 °C for 1, 5 and 20 h. It is important to point out again that the porosity of the coatings was measured via SEM and image analysis at a magnification of 500 times. Each porosity value represents the average of 10 image analysis measurements. It is important to stress that the SEM (500× magnification) and image analysis techniques employed in this work are able to identify the larger coarse pores of thermal spray coatings. Therefore, fine pores in between piled-up splats were not discernable by the porosity measurements of this study.

Despite the fact that the average particle temperature of the nanostructured and conventional YSZ particles were similar, the level of coarse porosity in the as-sprayed nanostructured coating is twice that of the conventional one, even though the average particle velocity of the nanostructured YSZ was higher than that of the conventional particles. One of the main reasons for this result is probably related to the trimodal distribution of pores in the nanostructured coating, as discussed in Section 3.4.1 and observed in the differences between Figs. 3a and 4. The trimodal distribution of pores (originating from the powder structure—Fig. 2) of the nanostructured coating maximizes its porosity levels (Fig. 3), even if the nanostructured and conventional powder particles were sprayed at similar temperature levels.

It should be highlighted that the heat treatment did not change this trend, in fact, the difference in porosity levels between the two coatings increased with heat treatment time (Fig. 5). The conventional coating exhibited a slight lowering of its coarse porosity levels after 1 h of heat treatment and stabilized after that. However, based on measurements of thermal diffusivity and elastic modulus, which will be shown in Sections 3.7 and 3.8, it can be inferred that there would be continuous lowering of the fine porosity levels of the conventional coating even after 20 h of heat treatment at 1400 °C.

As previously stated, the SEM (500× magnification) and image analysis techniques are able to identify the larger coarse pores of the bimodal distribution of the conventional YSZ coatings, however, the porosity changes probably occurred more significantly at very microscopic levels (fine porosity). This type of phenomenon was already highlighted by McPherson, i.e., at high temperatures, changes in coarse porosity may be negligible but healing of the fine pores occurs [17,20]. Therefore, considering porosity, the conventional coating seems to have exhibited the typical behaviour of ceramic materials when submitted to high temperature environments.

On the other hand, the nanostructured YSZ coating exhibited a behaviour that defies "conventional wisdom", i.e., its coarse porosity levels (measured using the techniques and conditions described in this paper) began and continued to increase during heat treatment, even after an exposure of 20 h at 1400 °C (Fig. 5). The coarse porosity level of the nanostructured coating heat-treated for 20 h was 1.8 times that of the as-sprayed coating. This result is explained in the next section.

It is important to note that, as in the case for the conventional coating, porosity reduction probably occurred for the nanostructured coating at very microscopic levels (fine porosity), e.g., in between piled-up splats, and was not discernable by SEM and image analysis at magnifications of 500 times. This subject will be discussed in more detail in Sections 3.7 and 3.8.

It is important to point out that all this discussion concerning fine and coarse porosities and their evolution upon sintering is based on experimental results on ceramic thermal spray coatings described in previous papers by other authors on the fundamental nature of the microstructure and mechanical properties, and their variation at high temperatures [17,20]. Further research using techniques like mercury intrusion porosimetry (MIP) will have to be carried out to experimentally prove the hypothesis presented in this paper.

3.6. Microstructures of the heat-treated coatings

The microstructures of the nanostructured YSZ coatings heat-treated at 1400 °C for 1, 5 and 20 h can be found in Fig. 6. It is possible to observe that at the magnification for taking the photos (500×), the coarse porosity of the coatings (i.e., the area of the black-colored regions) increased with increasing heat treatment time (Figs. 5 and 6).

The microstructure of the as-sprayed nanostructured coating (Fig. 3) was described in Section 3.4.1 as a bimodal one, formed by (i) a matrix of previously molten YSZ particles surrounding (ii) previously semi-molten nanostructured YSZ particles, i.e., the nanozones. It is expected that both the matrix and the nanozones will exhibit the traditional sintering effects, i.e., densification and shrinking, upon exposure to high temperatures. However, one may imagine that the densification rates of the matrix will be lower than those of the nanozones, because the matrix is basically formed by the previously molten and currently resolidified particles, i.e., its inner structure already exhibits high density after resolidification from the molten state. On the other hand, the porous nanozones, due to the presence of nanostructured particles and porosity (i.e., high surface area—Fig. 3b), will be under a higher driving force for sintering and densification. Therefore, the large nanozones tend to densify/shrink at faster rates than those of the matrix, thereby increasing the area (volume) of the coarse pores during heat treatment (Figs. 5 and 6). This is a direct consequence of the trimodal porosity of the nanostructured coating discussed in Section 3.4.1.

Despite this sintering effect, regions that were identified as nanozones in the as-sprayed coating are observed at higher magnifications after 20 h of heat treatment (Fig. 7). It is possible to distinguish their original microstructural characteristics or remains (Fig. 7). Finely dispersed porosity zones are still present in the former nanozones after 20 h at 1400 °C. It is important to point out that not only the particle size, but also the density of the body to be sintered (i.e., the nanozones) play an important role during the densification process (among other factors). Therefore, very porous regions, despite exhibiting particles with nanostructural character (Fig. 3b), will not necessarily exhibit full densification upon sintering (Fig. 7). Fig. 7 also shows the effect of the higher sintering rates of the nanozones (compared to those of the matrix). It is possible to observe that the original nanozones shrank at higher rates upon sintering, thereby creating open voids within the matrix structure.

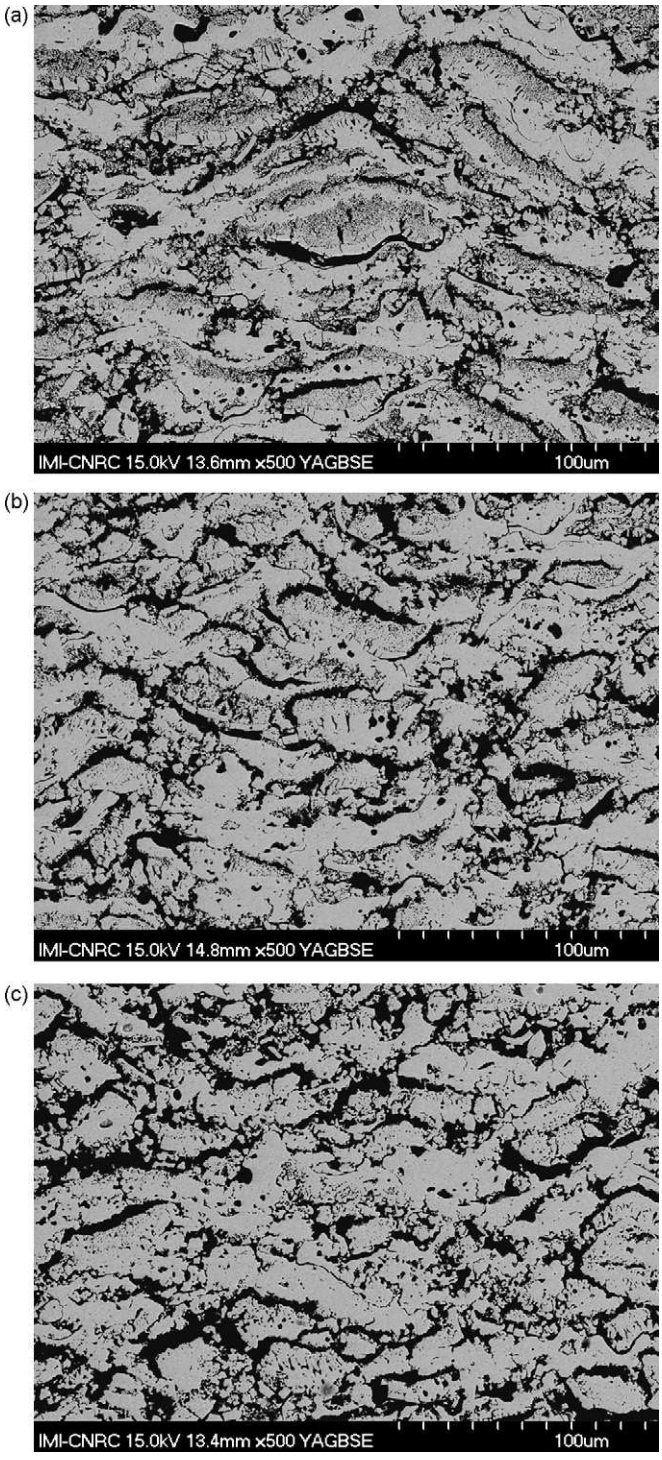

Fig. 6. Microstructures (cross-sections) of the nanostructured YSZ coating heat-treated at 1400 °C for (a) 1 h, (b) 5 h and (c) 20 h (scale bar: number represents combined distance across all tick divisions).

Fig. 8 shows the microstructure of the conventional YSZ coating after the heat treatment at 1400 °C for 20 h. Comparing this microstructure with that of the as-sprayed coating (Fig. 4), it is possible to observe some reduction in the area (volume) of coarse interlamellar pores, without a significant change in the amount of globular pores. This change was observed via SEM and image analysis (Fig. 5). It

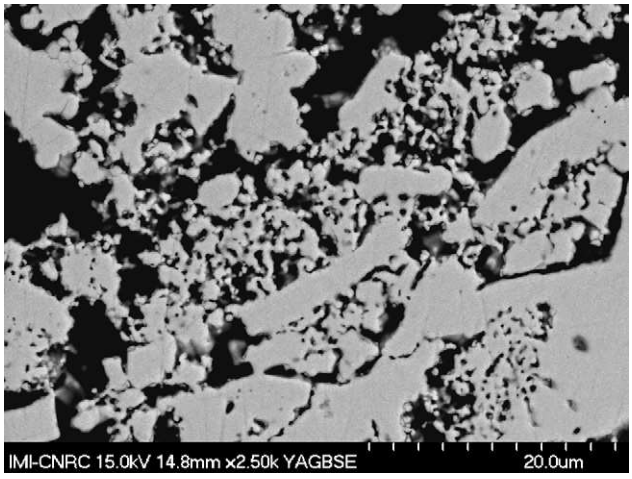

Fig. 7. Higher magnification view of the nanostructured YSZ coating heat-treated at 1400 °C for 20 h (Fig. 6c) (scale bar: number represents combined distance across all tick divisions).

seems to be fair to state that the microstructural changes in the conventional coating upon sintering were significantly lesser than those occurring with the nanostructured one (Figs. 3 and 6).

The following sections will show that these different microstructural changes will impart a significant difference of behaviour of thermal and mechanical properties of the two coatings after the heat treatment.

3.7. Thermal diffusivity

Fig. 9 shows the thermal diffusivity values for the as-sprayed and heat-treated nanostructured and conventional YSZ coatings. It is possible to observe that the as-sprayed thermal diffusivity value of the conventional YSZ coating is 57% higher than that of the nanostructured coating. The thermal diffusivity values of both coatings increase rapidly at 1400 °C after 1 h and the difference between them decreases to 45%. However, the

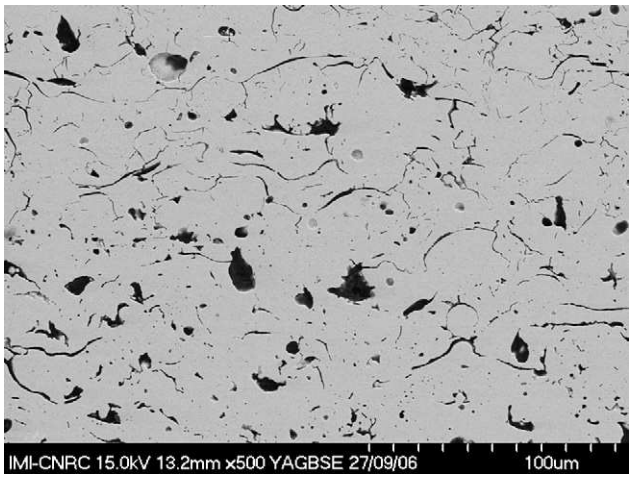

Fig. 8. Microstructure (cross-section) of the conventional YSZ coating heat-treated at 1400 °C for 20 h (scale bar: number represents combined distance across all tick divisions).

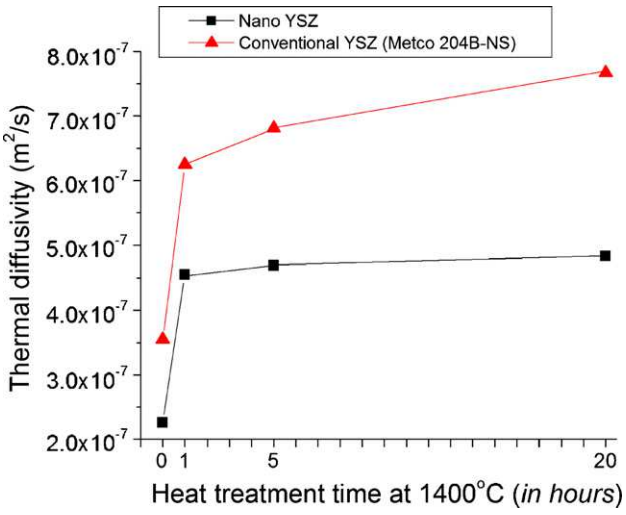

Fig. 9. Variation of the thermal diffusivity values from as-sprayed to heat-treated nanostructured and conventional YSZ coatings at 1400 °C for 1, 5 and 20 h.

thermal diffusivity value of the nanostructured coating basically stabilizes after 1 h of heat treatment, whereas, that of the conventional coating continues to increase with heat-treating time. After 20 h of heat treatment, the thermal diffusivity value of the conventional coating is 59% higher than that of the nanostructured coating and continues to increase.

It is hypothesized that the lower thermal diffusivity values of the as-sprayed nanostructured coating are strongly associated with its trimodal porosity (Fig. 3), because it maximizes the porosity levels of the coating as described in Sections 3.4.1 and 3.5. However, understanding the high temperature behaviour observed in Fig. 9 for the nanostructured coating is more complex. Based on the initial increase of thermal diffusivity values (after 1 h of heat treatment), it becomes evident that the nanostructured coating exhibited some degree of sintering, but according to Fig. 5, the porosity of this coating increased during heat treatment. It is hypothesized that during 1 h at 1400 °C, the fine interlamellar pores of the coating matrix exhibited significant healing, thereby increasing the thermal diffusivity values of the coating. As previously mentioned, these fine pores cannot be discerned by the image analysis measurements carried out in this work, and according to McPherson, they play a major role in the mechanical and thermal properties of thermal spray coatings [17,20].

On the other hand, after 1 h of heat treatment, sintering and densification of the nanozones became sufficiently effective to counteract the fine pore healing of the matrix by creating voids within the matrix structure, as observed and described in Figs. 5–7. It is important to point out that the scale bars of the cross-sections of Figs. 3, 4 and 6 are parallel to the substrate surface; therefore, the voids are creating a porosity that tends to be parallel to the substrate surface, being able to reduce heat transfer more effectively through the coating thickness. Therefore, as the healing of the fine interlamellar pores was counteracted by the formation of the horizontal voids in the nanostructured coating, its thermal diffusivity values tended to stabilize after 1 h of heat treatment at 1400 °C.

Table 1
Velocities of the acoustic waves generated via laser-ultrasonics in the as-sprayed and heat-treated nanostructured and conventional YSZ coatings

Condition	Acoustic wave velocity (m/s)	
	Nanostructured YSZ	Conventional YSZ
As-sprayed	907	2280
1400 °C/1 h	3403	3987
1400 °C/5 h	3482	4342
1400 °C/20 h	3661	4777

For the conventional coating, based on Figs. 4, 5 and 8, it is hypothesized that the pore healing occurred during the 20 h of heat treatment time. This behaviour is equivalent to that observed in other studies for YSZ coatings made from conventional powders [21,22]. As a consequence, its thermal diffusivity values continue to increase and have not reached a plateau even after 20 h at 1400 °C.

It is important to point out that sintering characteristics may also be affected by the degree of purity of a material, in addition to its microstructure and chemical composition. The individual nanostructured YSZ particles that formed the agglomerates (Fig. 2) were synthesized via a chemical method and precipitation, consequently, the degree of purity of this material tends to be high. Therefore, the evolution of the thermal diffusivity values of the nanostructured coating (Fig. 9) may have been affected by the purity of the powder in addition to its nanostructure.

As these coatings are to be applied as thermal barriers for protecting the metallic parts/components of gas turbines engines against the excessive heat generated by fuel combustion, the lower thermal diffusivity values of the nanostructured coating and their higher stabilities at high temperatures (when compared to the conventional one), are obvious advantages for employing the nanostructured material.

3.8. Elastic modulus

Table 1 shows the velocities of the acoustic waves generated via laser-ultrasonics for the as-sprayed and heat-treated nanostructured and conventional YSZ coatings. As stated in Section 2.5, the ultrasonic wave on the material is generated via a laser pulse. Each velocity value shown in Table 1 represents the average of 5–10 pulses. Each single laser pulse generates a signal that is detected by a second laser, located on the same surface but positioned away from the generating source of pulses. Based on the known distance between the source laser and the detection laser, and the time taken from the pulse generation to its detection, the velocity of the ultrasonic wave in the material is determined. Therefore, the velocities of Table 1 represent an average of 5–10 velocity measurements per coating.

In addition, in order to replicate measurements and test their reliability, each set of 5–10 velocity measurements was repeated twice, i.e., after the 1st set of values was obtained, the laser ultrasonics equipment was shut off, and each sample was turned 90° and a new series of sets of 5–10 measurements were taken. The maximum difference observed between average values was 2–3%. Therefore it is considered that the velocity measurements

of the acoustic waves obtained in his work were replicable and reliable, and the coatings showed no signs of in-plane anisotropy.

By looking at Table 1 it is possible to observe that the velocities of the waves on the nanostructured coatings are lower than those in the conventional ones. The elastic modulus value (E) of a material is directly proportional to its density (ρ) and the velocity (v) of the acoustic wave to the square travelling in the material ($E = \rho v^2$) [14]. By looking at the microstructures of the nanostructured (Figs. 3 and 6) and conventional YSZ (Figs. 4 and 8) coatings, and the coarse porosity values (Fig. 5), it is possible to infer that the nanostructured coatings exhibit lower density levels than those of the conventional ones. Therefore, the lower density levels of the nanostructured coatings and the lower wave velocities in their structures indicate that these coatings exhibit lower elastic modulus values than those of the conventional YSZ coatings. In order to make a relative comparison of elastic modulus values, as indicated in Section 2.5, a coating density of 4.7 g/cm^3 was employed for all coatings.

The theoretical density of the TBC material composition used in this work is estimated to be 5.7 g/cm^3. Therefore, the value of 4.7 g/cm^3 represents coatings having a porosity level of 18%. It must be stressed that this value is an estimated level of porosity and will yield relative values for elastic modulus that allow comparison of the coatings. Differences in the true density levels of the coatings will lead to the introduction of errors in these results. Ongoing work is focused on investigating the true level and nature of the porosity in the various coatings. Results from these ongoing studies, to be published later, will be used to provide a more fundamental understanding of differences between the nanostructured and conventional coatings and of the changes caused by heat treatment. General observations of the dimensional changes of the various coatings have led to the belief that major changes in the overall (bulk) density are not occurring during heat treatment. Although, shown in Section 3.5, measurements of coarse porosity made using image analysis indicated increasing levels of coarse porosity in nanostructured coatings during heat treatment, it is believed this coarse porosity replaced fine porosity that tended to disappear during heat treatment. This is an ongoing work, and more precise density and porosity measurements will be carried out by using techniques like MIP.

Fig. 10 shows the results for the elastic modulus values of the as-sprayed and heat-treated nanostructured and conventional YSZ coatings, if the density value of the coatings was fixed at 4.7 g/cm^3. These results represent relative elastic modulus values measured in the C_{11} in-plane direction, i.e., not through thickness. Elastic modulus values (in-plane) of as-sprayed YSZ coatings measured via different methods (laser-ultrasonics, Knoop indentation, Hertzian indentation, tensile method, four-point bending, cantilever beam and flexural resonance) have been reported in the literature [5,21,23–31]. The majority of these values were generally found in a range from ~20 to 50 GPa, i.e., the as-sprayed values of the YSZ coating of this study are also found within this range (Fig. 10).

After 1 h of heat treatment at 1400 °C, both values of elastic modulus have shown a marked increase from their as-sprayed ones, however, after this stage the elastic modulus values of the nanostructured coating tend to stabilize, whereas, those of the conventional coating continue to increase. After 20 h of heat treatment, the relative elastic modulus value of the conventional coating is significantly higher than that of the nanostructured one, i.e., the difference between the elastic modulus values continues to increase.

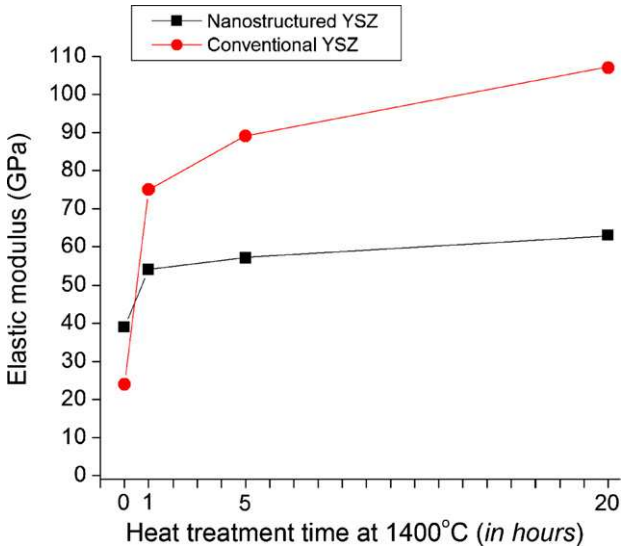

Fig. 10. Relative variation of the elastic modulus values from as-sprayed to heat-treated nanostructured and conventional YSZ coatings at 1400 °C for 1, 5 and 20 h (if the density value of the coatings was fixed at 4.7 g/cm^3).

The explanation of this phenomenon is basically the same one used to explain the thermal diffusivity behaviour, i.e., the presence of the porous nanozones in the coating will tend to form voids within the coating microstructure, arising from the differential sintering between the nanozones and the matrix, counterbalancing the densification effects caused due to the sintering of the nanozones and pore healing in the matrix (Figs. 3, 5–7).

The characteristics observed for the conventional coating are equivalent to those observed for the thermal diffusivity, i.e., it is hypothesized that the coating exhibited pore healing during the 20 h of heat treatment time. As a consequence, its elastic modulus values continue to increase and have not reached a plateau after 20 h at 1400 °C.

These results for elastic modulus have important implications for gas turbine applications. Because these coatings undergo thermal cycling in operation, materials with lower stiffness levels, such as the nanostructured coating reported in this study, have a distinct advantage due to their higher compliance characteristics in these situations.

It is important to point out again the values of elastic modulus reported in Fig. 10 must not be taken as absolute; rather, the data allows comparison of the different coatings and provides a basis for determining the relative effect of the various heat treatments on the elastic properties. In fact, it appears that the level of porosity in the nanostructured YSZs is higher than that in the conventional ones. If that is found to be the case, the difference in the calculated values of elastic modulus for the nanostructured and conventional coating will be even more pronounced than that shown in Fig. 10.

3.9. Highly sintering-resistant nanostructured YSZ TBC

The nanostructured YSZ coating engineered in this study counteracts sintering effects. Conventional materials are normally either inert to the environment in which they operate or undergo changes in reacting with the environment that generally have a negative impact on their performance and stability. An example of such a material is the conventional YSZ coating of this study. Its thermal diffusivity and elastic modulus values continue to increase after 20 h of heat exposure, an effect that is detrimental to its performance as a TBC.

The nanostructured YSZ coating engineered in this study reacts to the high temperature environment so that differential sintering rates between the matrix and nanozones prevent a steep continuous increase of thermal diffusivity and elastic modulus values over time.

4. Conclusions

In this study, nanostructured and conventional (HOSP) YSZ powder particles were thermally sprayed via APS. The produced coatings were heat-treated in air at 1400 °C for 1, 5 and 20 h. The microstructural characteristics, porosity, thermal diffusivity and elastic modulus values of the as-sprayed and heat-treated coatings were evaluated. The main conclusions are the following:

- The nanostructured YSZ coating was engineered to exhibit a bimodal distribution in its microstructure, which was formed by (i) previously molten and resolidified YSZ particles (matrix) that surrounded (ii) previously semi-molten porous nano YSZ agglomerates (nanozones) that were embedded in the coating microstructure during thermal spraying. The percentage of nanozones embedded in the coating structure was approximately 35%.
- The coarse porosity levels of the nanostructured coating increased during the heat treatment. After 20 h at 1400 °C, the coarse porosity level of the nanostructured coating was 3.5 times higher than that of the conventional one.
- This uncommon behaviour occurs due to the different sintering rates of the matrix and nanozones that form the nanostructured coating. The nanozones, due to their higher surface area, exhibit a higher driving force for sintering, thereby shrinking at much faster rates than those of the matrix and creating voids (coarse pores) within the coating structure upon high temperature exposure.
- The as-sprayed thermal diffusivity value of the conventional coating is ∼60% higher than that of the nanostructured one, a difference that is maintained even after a heat treatment at 1400 °C for 20 h. The relative elastic modulus value of the conventional coating after 20 h at 1400 °C is significantly higher than that of the nanostructured one. These effects are highly associated with the porosity evolution in both coatings.
- The nanostructured YSZ coating developed in this study reacts to the high temperature environment in such a way that differential sintering rates prevent steep continuous increase of thermal diffusivity and elastic modulus values over time. This study demonstrates that nanostructured YSZ coatings can be engineered to counteract sintering effects and exhibit significantly lower increases in thermal diffusivity and elastic modulus values in high temperature environments when compared to those of conventional YSZ coatings. A series of other tests are planned to verify the effectiveness of these nano YSZ coatings for TBC applications; however, the results reported in this study are considered very promising.

Prime novelty statement

Thermal sprayed nanostructured ZrO_2–7 wt% Y_2O_3 (YSZ) coatings were engineered to counteract sintering effects. The use of nanostructured YSZ coatings represents an alternative to improving the performance of thermal barrier coatings (TBCs). However, there are still fundamental questions to be answered on the applicability of nanostructured YSZ coatings as TBCs. These questions are related to sintering effects, which could significantly increase the thermal diffusivity/conductivity and elastic modulus values of these types of coatings in high temperature environments. Nanostructured and conventional YSZ thermal spray coatings were heat treated in air at 1400 °C for 1, 5 and 20 h. Due to using the concept of differential sintering rates, nanostructured YSZ coatings exhibited much lower increase of thermal diffusivity and elastic modulus values than those exhibited by a conventional YSZ coating.

Acknowledgements

The authors would like to thank the collaboration and discussions of Dr. S.E. Kruger concerning the elastic modulus measurements of the YSZ coatings via laser-ultrasonics. Special thanks to S. Bélanger for producing the coatings via APS, B. Harvey for sample preparation, F. Belval for heat treatment, M. Lamontagne for the Accuraspray and thermal diffusivity measurements, J.-F. Alarie for metallography and M. Thibodeau for SEM pictures and image analysis.

References

[1] R.A. Miller, Surf. Coat. Technol. 30 (1987) 1–11.
[2] N.P. Padture, M. Gell, E.H. Jordan, Science 296 (2002) 280–284.
[3] C.C. Koch, Nanostructured Materials—Processing, Properties and Applications, Noyes Publications, William Andrew Publishing, Norwich, NY, USA, 2002.
[4] R.S. Lima, B.R. Marple, J. Therm. Spray Technol. 16 (1) (2007) 40–63.
[5] R.S. Lima, A. Kucuk, C.C. Berndt, Surf. Coat. Technol. 135 (2001) 166–172.
[6] R.S. Lima, A. Kucuk, C.C. Berndt, Mater. Sci. Eng. A 313 (2001) 75–82.
[7] R.S. Lima, A. Kucuk, C.C. Berndt, Mater. Sci. Eng. A 327 (2002) 224–232.
[8] M.R. Gold, R.S. Lima, A. Kucuk, C.C. Berndt, Scratch Testing and Acoustic Emission of Nanostructured Partially Stabilized Coatings, in: K. Ravi-Chandar, B.L. Karihaloo, T. Kishi, R.O. Ritchie, A.T. Yokobori Jr., T. Yokobori (Eds.), Proceedings of the 10th International Conference on Fracture, Pub. Elsevier Science, Oxford, 2001 (Paper #ICF1001074, pdf format).
[9] B. Liang, C. Ding, Surf. Coat. Technol. 197 (2005) 185–192.
[10] W.Q. Wang, C.K. Sha, D.Q. Sun, X.Y. Gu, Mater. Sci. Eng. A 424 (2006) 1–5.

[11] R.S. Lima, B.R. Marple, C. Moreau, Thermal Spray Coating of Porous Nanostructured Ceramic Feedstock, USA and PCT patent pending, 2006 (NRC file 11810-1).
[12] B.R. Marple, R.S. Lima, C. Moreau, S.E. Kruger, L. Xie, M. Dorfman, in: B.R. Marple, M.M. Hyland, Y.-C. Lau, C.-J. Li, R.S. Lima, G. Montavon (Eds.), Processing and Properties of Yttria-Stabilized Zirconia TBCs Produced Using Nitrogen as Primary Plasma Gas, Thermal Spray 2007: Global Coating Solutions, ASM International, Materials Park, OH, USA, 2007, pp. 405–410.
[13] A.S. Houlbert, P. Cielo, C. Moreau, M. Lamontagne, Int. J. Thermophys. 15 (3) (1994) 525–546.
[14] R.S. Lima, S.E. Kruger, G. Lamouche, B.R. Marple, J. Therm. Spray Technol. 14 (1) (2005) 52–60.
[15] J.-F. Bisson, C. Moreau, M. Dorfman, C. Dambra, J. Mallon, J. Therm. Spray Technol. 14 (1) (2005) 85–90.
[16] K. Muraleedharan, J. Subrahmanyam, S.B. Bhaduri, J. Am. Ceram. Soc. 71 (5) (1988) C226–C227.
[17] R. McPherson, Surf. Coat. Technol. 39/40 (1989) 173–181.
[18] A. Kucuk, R.S. Lima, C.C. Berndt, J. Am. Ceram. Soc. 84 (4) (2001) 685–692.
[19] H.E. Eaton, P. Zajchowski, Surf. Coat. Technol. 120/121 (1999) 28–33.
[20] R. McPherson, Thin Solid films 112 (1984) 89–95.
[21] A. Kulkarni, A. Vaidya, A. Goland, S. Sampath, H. Herman, Mater. Sci. Eng. A 359 (2003) 100–111.
[22] F. Cernuschi, L. Lorenzoni, S. Ahmaniemi, P. Vouristo, T. Mantyla, J. Eur. Ceram. Soc. 25 (2005) 393–400.
[23] D.L. Vasquez, A. Kucuk, R.S. Lima, U. Senturk, C.C. Berndt, in: C.C. Berndt, K.A. Khor, E.F. Lugscheider (Eds.), Elastic Modulus Measurements of Air Plasma Sprayed Yttria Partially Stabilized Zirconia Coatings Using Laser Ultrasonics and Indentation Techniques, Thermal Spray 2001: New Surfaces for a New Millenium, ASM International, Materials Park, OH, USA, 2001, pp. 1045–1050.
[24] E.F. Rybicki, J.R. Shadley, Y. Xiong, D.J. Greving, J. Therm. Spray Technol. 4 (4) (1995) 377–383.
[25] H.-D. Steffens, U. Fischer, in: D.L. Houck (Ed.), Correlation Between Microstructure and Physical Properties of Plasma Sprayed Zirconia Coatings, Thermal Spray: Advances in Coatings Technology, ASM International, Materials Park, OH, USA, 1988, pp. 167–173.
[26] S.-H. Leigh, C.-K. Lin, C.C. Berndt, J. Am. Ceram. Soc. 80 (8) (1997) 2093–2099.
[27] J.S. Wallace, J. Ilavsky, J. Therm. Spray Technol. 7 (4) (1998) 521–526.
[28] T. Hilpert, E. Ivers-Tiffée, Solid State Ionics 175 (2004) 471–476.
[29] M. Eskner, R. Sandstrom, Surf. Coat. Technol. 177/178 (2004) 165–171.
[30] H. Guo, S. Kuroda, H. Murakami, J. Am. Ceram. Soc. 89 (4) (2006) 1432–1439.
[31] S. Ahmaniemi, P. Vuoristo, T. Mantyla, Mater. Sci. Eng. A 366 (2004) 175–182.